Journal of
Applied
Crystallography
ISSN 0021-8898

Received 10 January 2012
Accepted 31 May 2012

Real-time synchrotron X-ray diffraction study on the isothermal martensite transformation of maraging steel in high magnetic fields

D. San Martin,[a] E. Jiménez-Melero,[b,c] J. A. Duffy,[d] V. Honkimäki,[e] S. van der Zwaag[f] and N. H. van Dijk[b]*

[a]MATERALIA Group, Department of Physical Metallurgy, Centro Nacional de Investigaciones Metalúrgicas (CENIM-CSIC), Avenida Gregorio del Amo 8, 28040 Madrid, Spain, [b]Fundamental Aspects of Materials and Energy, Faculty of Applied Sciences, Delft University of Technology, Mekelweg 15, 2629 JB Delft, The Netherlands, [c]Dalton Cumbrian Facility, University of Manchester, Westlakes Science and Technology Park, Moor Row, Cumbria CA24 3HA, UK, [d]Department of Physics, University of Warwick, Coventry CV4 7AL, UK, [e]European Synchrotron Radiation Facility, 6 rue Jules Horowitz, BP 220, 38043 Grenoble, France, and [f]Novel Aerospace Materials, Faculty of Aerospace Engineering, Delft University of Technology, Kluyverweg 1, 2629 HS Delft, The Netherlands. Correspondence e-mail: n.h.vandijk@tudelft.nl

The isothermal austenite-to-martensite transformation kinetics in a maraging steel have been studied by time-dependent microbeam diffraction measurements with high-energy X-rays. The transformation kinetics are shown to be accelerated significantly when a magnetic field of 8 T is applied. The average phase behaviour, obtained from a Rietveld refinement of the powder-averaged diffraction data, demonstrates that the martensite formation does not lead to a macroscopic strain in the austenite and martensite phases. An analysis of individual austenite reflections in the microbeam diffraction patterns, however, indicates that within the transforming austenite grains a transformation strain develops as a result of the formed martensite. The development of elastic strains during the transformation is explained by a partial strain confinement within the untransformed part of the austenite grain. The strain relaxation to the surrounding austenite grains is found to be dependent on the austenite volume. For a set of individual austenite grains the martensite nucleation is correlated with the initial austenite volume and the strain developed prior to the transformation as a result of martensite formation in the neighbouring grains.

1. Introduction

Maraging steels form a class of low-carbon high-alloyed steels developed in the 1960s for applications requiring ultra-high strength combined with good fracture toughness and corrosion resistance. Their remarkable properties are obtained through a process of martensite formation followed by an age-hardening treatment to form fine precipitates in the martensitic matrix (Slunder *et al.*, 1968). For some maraging steels the martensite can be formed by an isothermal phase transformation below room temperature (Holmquist *et al.*, 1995; San Martin *et al.*, 2010). The time-dependent formation of martensite at a constant temperature was first observed by Kurdjumov & Maksimova (1948, 1950) in an Fe–Mn alloy and has subsequently been reported for several other systems, such as Fe–Ni–Cr and Fe–Ni–Mn alloys (Kakeshita *et al.*, 1993*a*; Borgenstam & Hillert, 1997). More recently, isothermal time-dependent martensite formation has also been observed in other metal alloys (Sordelet *et al.*, 2007; Jeffries *et al.*, 2009*a*,*b*; Kustov *et al.*, 2010; Lee *et al.*, 2011) and ceramics (Pee *et al.*, 2006). In all these systems the martensite fraction depends on both time and temperature. In contrast, for the more common athermal martensitic transformations the martensite fraction is independent of time and only governed by the lowest temperature reached (Porter *et al.*, 2009).

The isothermal transformation from the austenite phase (γ), with a face-centred cubic structure, into the martensite phase (α'), with a body-centred cubic structure, is associated with an experimental C-curve kinetics with a maximum transformation rate at the so-called nose temperature. In Fig. 1 the time evolution of the corresponding microstructure is illustrated. The proposed models for the isothermal martensitic transformation (Kakeshita *et al.*, 1993*b*; Ghosh & Olson, 1994; Borgenstam & Hillert, 1997) have so far not been able to unravel the martensite nucleation mechanism in detail. Experimentally it was found that the martensite formation not only is a function of time and temperature, but also can be assisted by magnetic fields. In the presence of an applied magnetic field the transformation from the paramagnetic austenite phase into the ferromagnetic martensitite phase is promoted. In recent time-dependent magnetization measure-

ments on maraging steel we monitored the evolution of the martensite phase fraction in magnetic fields up to 9 T (San Martin *et al.*, 2008) and 30 T (San Martin *et al.*, 2010) for a wide range of temperatures. It was observed that the transformation rate can be enhanced significantly in the presence of high magnetic fields. Other recent studies focused on the influence of high magnetic fields on diffusional phase transformations in steel (Ohtsuka *et al.*, 2000; Joo *et al.*, 2000; Guo & Enomoto, 2000; Enomoto *et al.*, 2001; Zhang *et al.*, 2004; Jaramillo *et al.*, 2005; Rivoirard *et al.*, 2006).

In order to study the isothermal martensite transformation in maraging steel we performed microbeam synchrotron X-ray diffraction measurements with high-energy X-rays (80 keV) in zero field and in a magnetic field of 8 T. These *in situ* X-ray diffraction experiments have allowed us to study simultaneously the overall martensite formation and the transformation behaviour of individual metastable austenite grains within the bulk of the material. Only with the help of a high magnetic field could the transformation kinetics be monitored within realistic time scales. A constant temperature of 233 K (nose temperature) was adopted to achieve a maximum transformation rate (San Martin *et al.*, 2010). To our knowledge the reported synchrotron experiments are the first *in situ* X-ray diffraction measurements on the isothermal martensite formation in maraging steels. Previous synchrotron X-ray diffraction studies on maraging steel (Hedström *et al.*, 2007; Zickler *et al.*, 2009; Schnitzer *et al.*, 2010) were devoted to the time-independent deformation behaviour, while small-angle X-ray scattering (Servant *et al.*, 1987) and small-angle neutron scattering (Staron *et al.*, 2003) studies have monitored the nanoscale precipitation behaviour during the final age-hardening treatment. In earlier time-resolved microbeam X-ray diffraction studies we have probed the transformation kinetics during diffusion-controlled solid-state phase transformations (Offerman *et al.*, 2002) and solidification (Iqbal *et al.*, 2005) at a single-grain level.

2. Experimental

2.1. Samples

The composition of the studied metastable austenitic maraging steel was 12 Cr, 9 Ni, 4 Mo, 2 Cu, 1 Ti, 0.7 Al, 0.3 Mn, 0.3 Si, <0.01 C, N and balance Fe (in wt%). The samples were heated to 1223 K, kept for 10 s and cooled to room temperature at 900 K min^{-1} using a vacuum furnace to obtain a fully austenitic microstructure. During the isothermal martensitic transformation the paramagnetic austenite phase γ transformed progressively into the ferromagnetic martensite phase α'. For this steel the formation of martensite is accompanied by an increase in volume of $\Delta V/V \simeq 2\%$, and an age-hardening heat treatment results in the formation of the χ phase (Lai *et al.*, 2004; San Martin *et al.*, 2007, 2008). This χ phase ($Fe_{36}Cr_{12}Mo_{10}$) is paramagnetic and forms as fine precipitates. For the studied samples, where no final ageing was applied, the presence of nano-sized χ-phase precipitates was not observed within the experimental resolution.

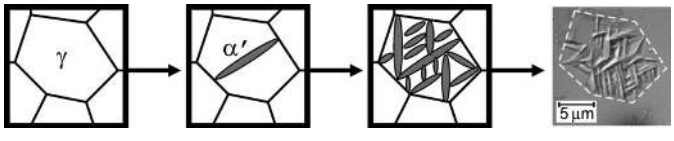

Figure 1
Schematic view of the microstructure evolution during the isothermal transformation from austenite (γ) into martensite (α'), together with an optical micrograph of the surface roughening resulting from the transformation (San Martin *et al.*, 2007). The dashed line indicates the original austenite grain boundaries.

2.2. *In situ* high-energy X-ray diffraction

The isothermal formation of martensite in maraging steel was studied by means of *in situ* high-energy X-ray diffraction. The experiment was performed at beamline ID15A of the European Synchrotron Radiation Facility (Grenoble, France). In Fig. 2 a schematic representation of the setup used for the experiment is displayed. Plate samples with a thickness of 0.45 mm were mounted in an 8 T cryomagnet (Oxford Instruments) placed on an *XYZ* translation table that allowed translations in three dimensions in space, together with ω rotations around the vertical sample axis. The horizontal magnetic field was applied perpendicular to the sample plate and for a sample rotation of $\omega = 0^\circ$ oriented along the X-ray beam. The sample was illuminated with an intense monochromatic X-ray beam with an energy of 80 keV ($\lambda = 0.155$ Å) using two different beam sizes of 44 × 44 and 60 × 60 μm. The sample (together with the horizontal field) was continuously rotated around its cylindrical axis in steps of $\Delta\omega = 0.4^\circ$, covering a total ω range from -1.6 to $+1.6^\circ$ (eight steps). During each of these steps in ω, the diffracted intensity was simultaneously collected on the two-dimensional CCD

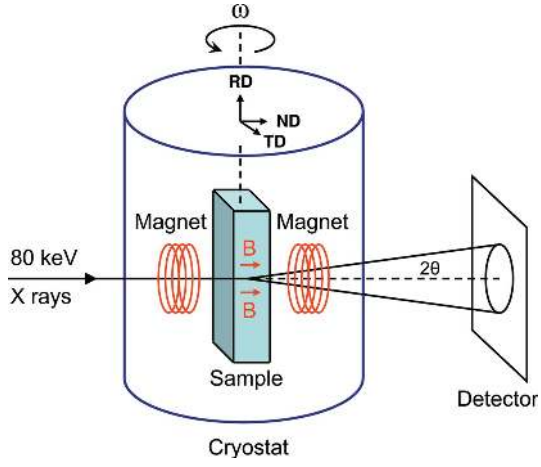

Figure 2
Layout of the synchrotron X-ray diffraction setup. The sample is placed in a cryostat with a horizontal magnetic field applied along the beam. The sample and cryostat are rotated along the vertical axis (ω rotation) during exposure. The diffracted intensity is recorded on a two-dimensional detector placed behind the sample (transmission geometry). The sample principle directions (rolling direction, normal direction and transverse direction), RD, ND and TD, are indicated.

detector (mar) placed behind the sample. The exposure time for each diffraction pattern was t_{exp} = 5 s. The sample-to-detector distance and the energy of the X-ray beam were calibrated using a high-purity iron powder sample. The magnetic field was applied as soon as the sample temperature of 233 K had been reached.

2.3. Data analysis

The measured data consisted of a series of two-dimensional diffraction patterns as a function of time, beam size and ω angle. To study the average phase behaviour the two-dimensional diffraction patterns for the largest beam size were summed over the covered ω range. Afterwards, an integration over all azimuth angles at constant scattering angle was performed using the *FIT2D* software package (Hammersley *et al.*, 1996) to obtain the corresponding one-dimensional diffraction patterns (intensity *versus* scattering angle). A Rietveld refinement of the resulting one-dimensional X-ray diffraction patterns was performed in sequential mode using the *Fullprof* package (Rodríguez-Carvajal, 1993) in order to determine the phase fraction and lattice parameters of the austenite and martensite phases as a function of time.

A single-grain analysis was performed on individual diffraction spots to characterize the (untransformed) volume, the lattice parameter and the orientation of the diffracting planes for the monitored austenite grains. The austenite volume is obtained from the peak intensity integrated over the sample rotation angle. By comparing the integrated intensity for the two different beam sizes we could check whether the grain was fully illuminated by the smaller beam size during the experiment. The lattice parameter and orientation of the diffraction plane normal was obtained from an evaluation of the peak position on the two-dimensional detector. The data analysis method was described in detail elsewhere (Jimenez-Melero, van Dijk, Zhao, Sietsma, Offerman *et al.*, 2007; Jimenez-Melero, van Dijk, Zhao, Sietsma & van der Zwaag, 2007).

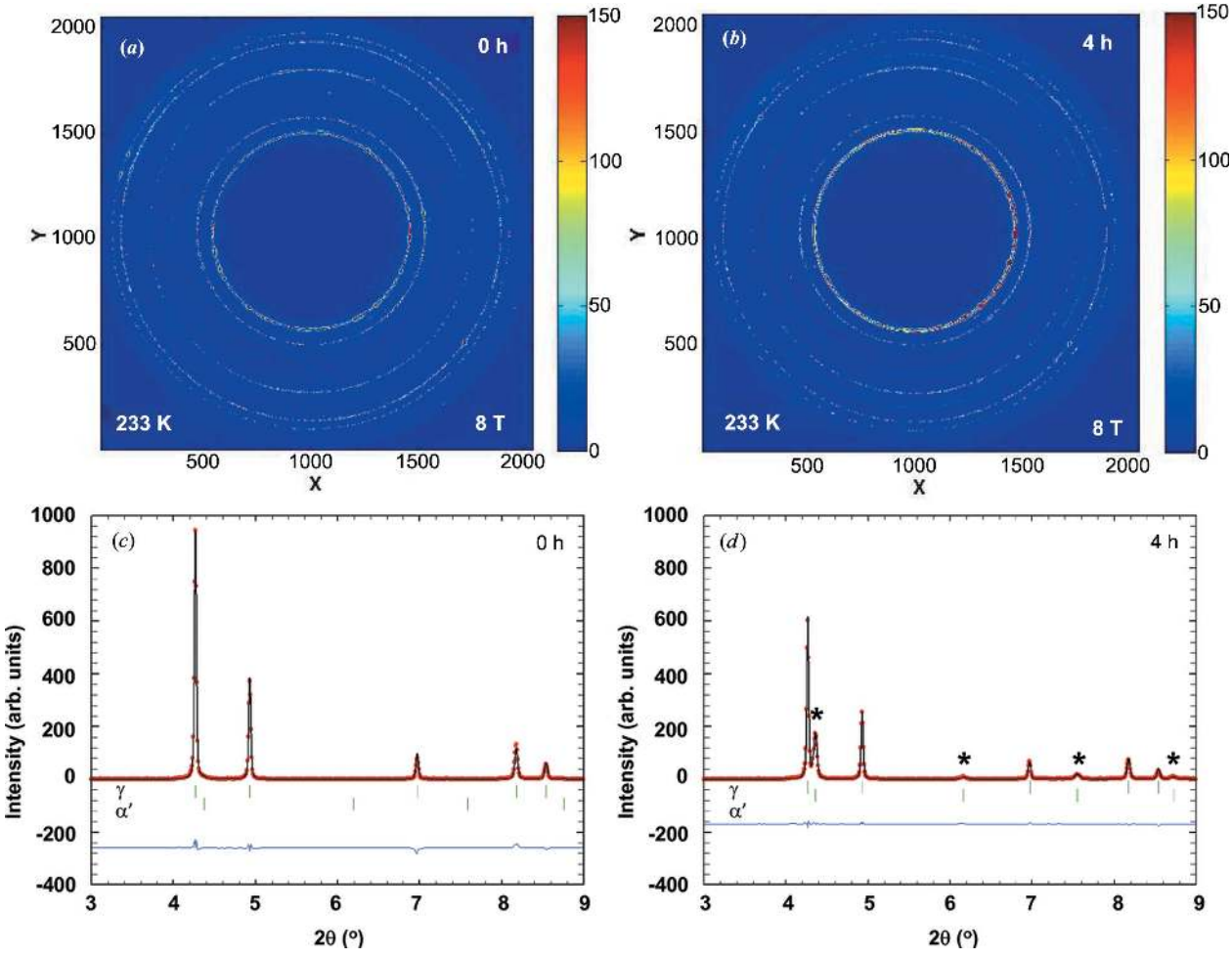

Figure 3
Two-dimensional synchrotron X-ray diffraction pattern of maraging steel for an isothermal martensite transformation time of t = 0 (*a*) and t = 4 h (*b*) at 233 K in a magnetic field of 8 T (summed over the total rotation angle of 3.2° for a beam size of 60 × 60 µm). The corresponding diffracted intensity as a function of scattering angle 2θ is shown for a transformation time of t = 0 (*c*) and t = 4 h (*d*). The pattern at 0 h corresponds to the original austenite phase (γ), while the stars at 4 h indicate the reflections from the newly formed martensite phase (α').

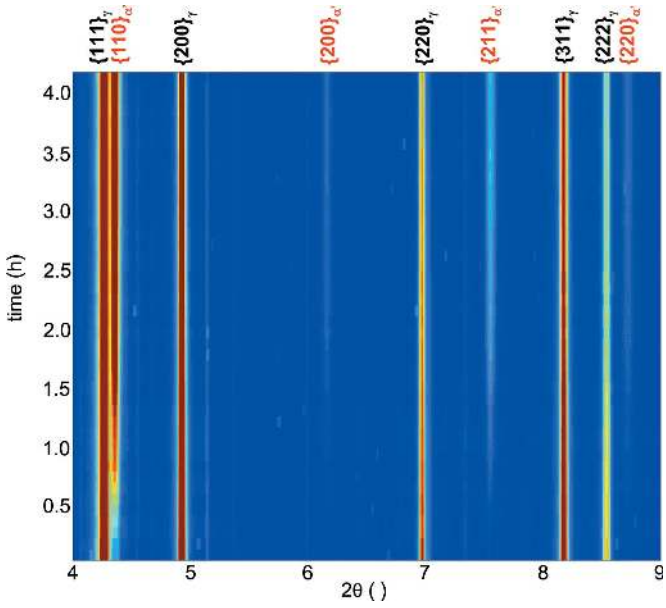

Figure 4
Time evolution of the diffracted X-ray intensity of maraging steel as a function of scattering angle 2θ during the isothermal martensite transformation at 233 K in an applied magnetic field of 8 T. The position of the monitored $\{hkl\}$ reflections is indicated for the untransformed austenite (γ) and the formed martensite (α').

3. Results

3.1. Average phase behaviour

In Fig. 3 the two-dimensional diffraction pattern of the studied maraging steel summed over the total rotation angle of 3.2° is shown (*a*) at the start of the isothermal martensitic transformation and (*b*) after a transformation time of 4 h at a temperature of 233 K and in an applied magnetic field of 8 T. The corresponding one-dimensional diffraction patterns at constant scattering angle are shown in Figs. 3(*c*) and 3(*d*). A comparison of the data before and after 4 h of transformation clearly indicates a reduction in peak intensity for the austenite phase in combination with the appearance of new peaks originating from the newly formed martensite phase. In Fig. 4 the time evolution of the one-dimensional diffraction pattern (integrated over the covered rotation angle of 3.2°) is shown. A gradual increase in intensity is observed for the martensite peaks as the isothermal transformation proceeds. As expected, this increase in intensity of the martensite peaks coincides with a continuous decrease in intensity of the austenite peaks.

In Fig. 5 the time evolution of the phase fraction and the lattice parameters of the transforming austenite phase and the formed martensite phase are shown. In an applied magnetic field of 8 T a martensite volume fraction of about 40% was

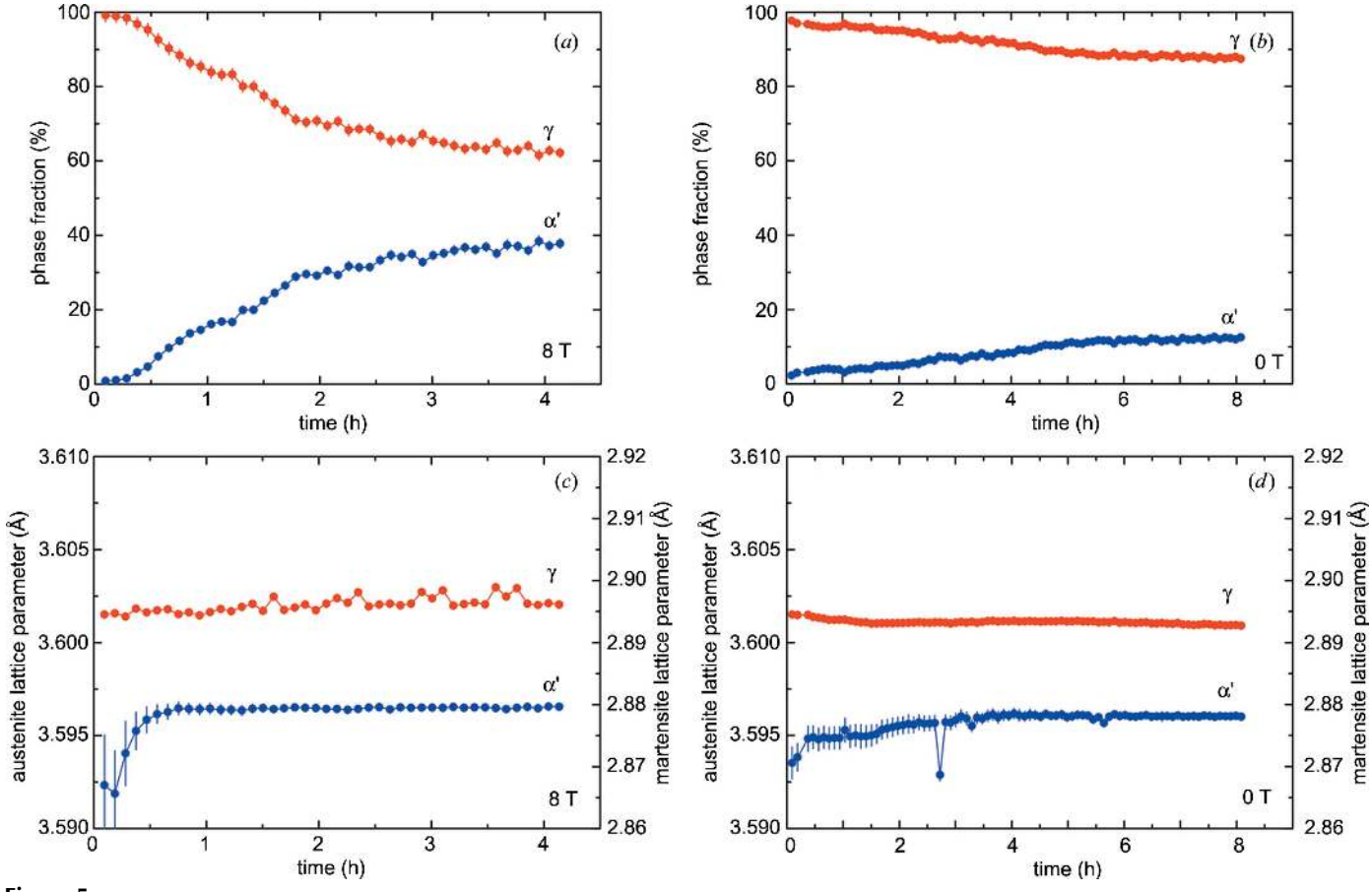

Figure 5
Fit results of the X-ray powder diffraction for maraging steel during the isothermal martensitic transformation at 233 K. The phase fractions of the untransformed austenite (γ) and the formed martensite (α') are shown as a function of the transformation time in a magnetic field of 8 T (*a*) and in zero field (*b*). The time evolution of the corresponding lattice parameters for austenite and martensite is shown for (*c*) 8 T and (*d*) zero field.

found for a transformation time of 4 h (Fig. 5*a*). In zero field a volume fraction of only 10% was observed after a transformation time of 8 h (Fig. 5*b*). This indicates that the applied magnetic field resulted in a significant acceleration of the isothermal martensitic transformation at a temperature of 233 K. The lattice parameters of austenite and martensite did not show a significant time evolution for either of the magnetic field conditions (Figs. 5*c* and 5*d*). The lattice parameter for martensite seemed to show a minor increase at the start of the transformation. However, for the small fraction transformed in this region the uncertainty in lattice parameter is considerable, which suggests that this initial variation might not be significant. Comparing the initial austenite lattice parameter of $a_\gamma = 3.6015\ (1)$ Å with the final martensite lattice parameter of $a_{\alpha'} = 2.8797\ (1)$ Å, obtained after 4 h of transformation in a field of 8 T, a relative volume change of 2.1% is obtained. The average phase strain developed in the austenite phase during the martensite transformation was found to be negligible with an upper bound of 0.02%.

3.2. Single-grain behaviour

In Fig. 6 an example is shown of an individual austenite diffraction peak on the two-dimensional detector at the start of the transformation to illustrate the analysis method. Each peak was monitored for a range of sample rotation angles ω and for two beam sizes. In order to obtain a reliable estimate of the austenite volume from the diffraction peak two validations need to be performed: (i) check that the grain is completely illuminated (the peak intensity should remain constant when the beam size increases) and (ii) check that the reflection is completely scanned within the probed angular rotation.

Using the previously developed method (Jimenez-Melero, van Dijk, Zhao, Sietsma, Offerman *et al.*, 2007; Jimenez-Melero, van Dijk, Zhao, Sietsma & van der Zwaag, 2007) to analyse validated single reflections, we have evaluated the volume, the lattice parameter and the orientation of the diffraction plane normal for about 100 individual austenite grains. The analysed individual austenite reflections appeared on the {111}, {200}, {220}, {311} and {222} diffraction rings on the two-dimensional detector. The behaviour of these single austenite grains was tracked as a function of time during the isothermal martensitic transformation at constant temperature (233 K) and magnetic field (8 T). The formed martensite consisted of very thin plates (50–100 nm thick) that could not be resolved as individual reflections in the current experiment.

The time evolution for the austenite volume of the individual austenite grains fell into two categories: nontransforming grains with a constant volume and transforming grains that show a reduction in austenite volume due to the martensite formation. In Fig. 7 the time evolution of the austenite volume and the strain is shown for some of the nontransforming austenite grains. Even though the austenite volume remained constant, the strain (obtained from the relative change in

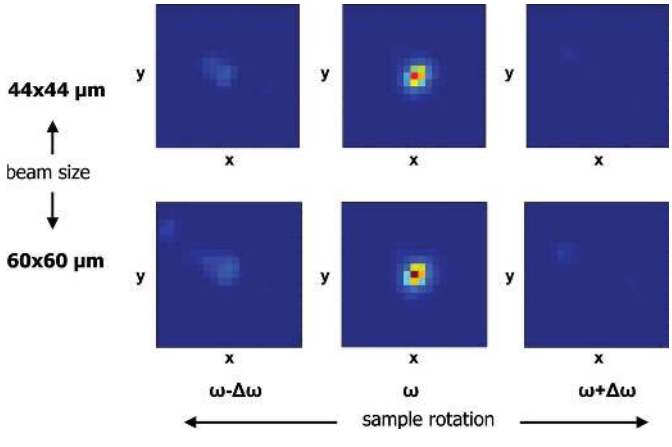

Figure 6
Example of an individual diffraction peak on the two-dimensional detector originating from an austenite grain at the start of the transformation. The peak was monitored for a range of sample rotation angles ω and for two beam sizes of 44 × 44 and 60 × 60 µm in order to collect the full integrated intensity and to verify that the grain was completely illuminated. During exposure the sample was continuously rotated over an angular range of $\Delta\omega = 0.4°$.

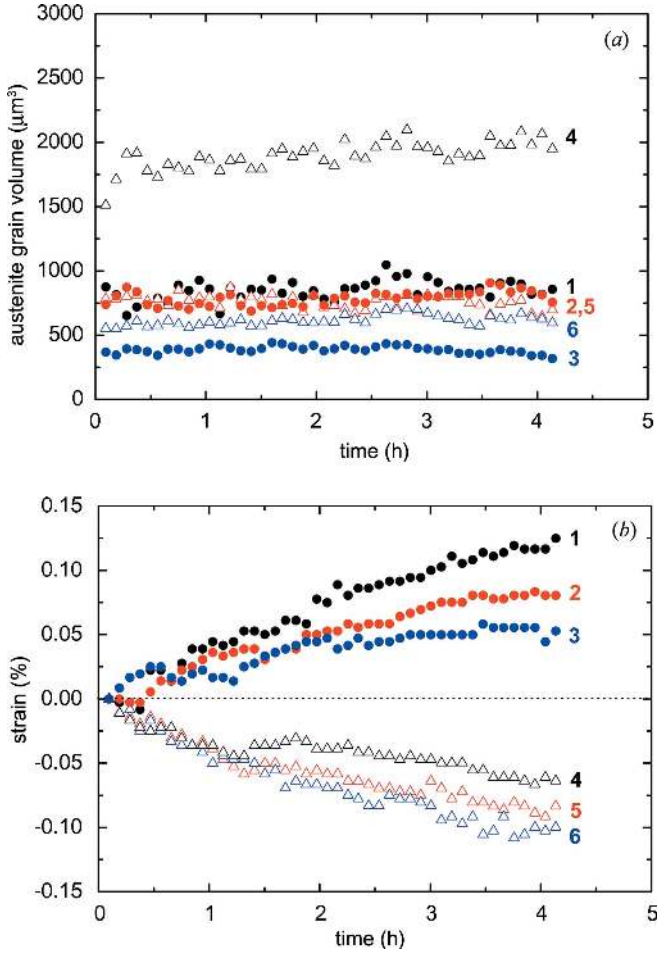

Figure 7
Time evolution of the austenite volume (*a*) and the elastic strain (*b*) for several nontransforming austenite grains during the isothermal martensite formation at 233 K in a magnetic field of 8 T. Each grain develops a continuously growing strain due to the martensite formation in neighbouring grains.

lattice parameter) showed a significant time evolution for individual austenite grains. This is remarkable as the average phase behaviour did not exhibit a significant strain development. As shown in Fig. 7, both positive and negative strains are found. The observed strains for the nontransforming austenite grains generally tend to grow continuously while the martensitic transformation is taking place in the neighbouring grains.

In Fig. 8 the time evolution of the austenite volume and the lattice parameter is shown for several transforming austenite grains during the martensitic transformation. The austenite volume remains constant until the first martensite plates are formed. When the transformation starts the austenite volume gradually decreases as more and more martensite plates are formed in the remaining austenite until the complete grain is transformed. The corresponding lattice parameter can

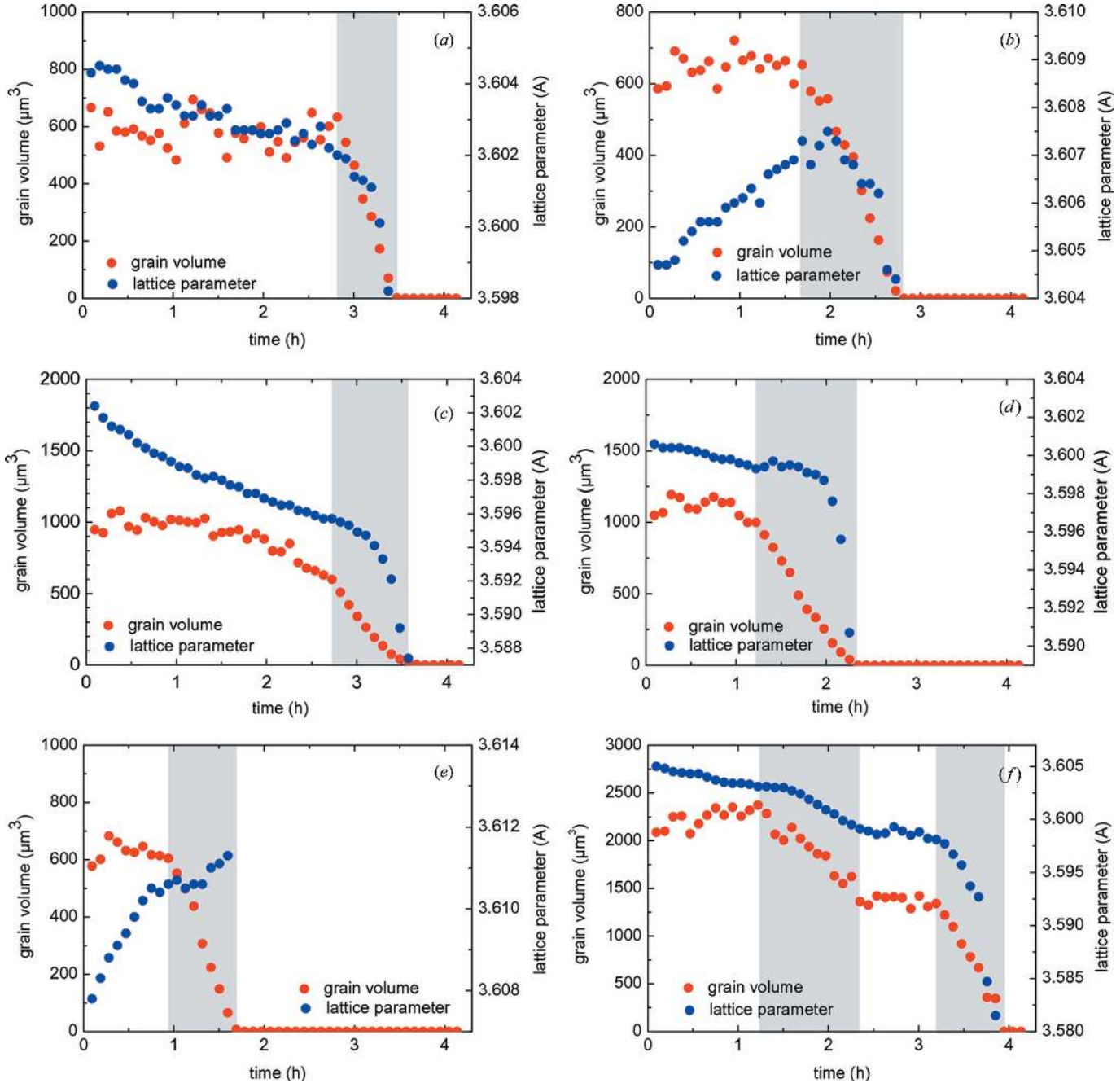

Figure 8
Time evolution of the austenite volume and the lattice parameter of several transforming austenite grains as a function of time at 233 K in a magnetic field of 8 T. Initially the austenite volume is constant, while during the martensitic transformation (grey region) the austenite volume gradually reduces until the complete austenite grain has transformed. During the martensitic transformation the austenite lattice parameter decreases as a result of the compressive transformation strain from the formed martensite.

increase or decrease before the start of the transformation. Once the martensite starts to form the austenite lattice parameter generally decreases owing to the compressive strain caused by the volume change resulting from austenite-to-martensite transformation. For larger grains the change in lattice parameter generally sets in later than the change in austenite volume.

In order to evaluate the martensite nucleation process during the isothermal transformation the martensite start time (t_{start}) was correlated with the initial austenite volume and the elastic strain prior to the transformation. In Fig. 9 the results are shown for the monitored individual austenite grains. For the transforming austenite grains, the martensite start time tends to be shorter for the larger grains. Remarkably, all grains nucleated before a (positive or negative) strain of about 0.12% was reached. For comparison, data for the nontransforming grains are also displayed at the top of the graphs. The grain orientation (plane normal) with respect to the applied magnetic field showed no significant influence on the martensite start time (data not shown).

4. Discussion

4.1. Development of elastic strains in nontransforming austenite grains

Fig. 7 shows that, in the nontransformed individual austenite grains, positive or negative strains gradually develop. A comparison with the average phase behaviour in Fig. 5, however, indicates that the austenite phase does not show a significant macroscopic strain up to an overall martensite fraction of 40%. Locally the 2.1% increase in volume associated with the austenite-to-martensite transformation will lead to a strain in the untransformed neighbouring austenite grains, but when averaged over the total sample volume, this strain is fully relaxed. Nontransforming austenite grains that are located close to a formed martensite plate (in a neighbouring austenite grain) are expected to experience a compressive strain. Austenite grains that are located at a further distance may then experience a tensile strain as a result of the macroscopic strain relaxation in the overall structure.

4.2. Transformation behaviour of austenite grains

In Fig. 8 the characteristic transformation behaviour is shown for several individual austenite grains. In this plot the time evolution of the austenite volume and the austenite lattice parameter are shown. In all cases the transformation takes place in the form of a gradual decrease in austenite volume. This indicates that the present time resolution is insufficient to see a stepwise reduction in volume due to the progressive formation of individual martensite plates. Before the transformation starts to take place within an austenite grain, the lattice parameter can show a significant time evolution as a result of transformation events in neighbouring grains. When the transformation sets in within the monitored grain the lattice parameter generally shows a reduction due to the compressive transformation strain (the formed martensite has a larger volume).

The following main transformation types can be observed: (i) direct response (Figs. 8*a* and 8*b*), (ii) delayed response (Figs. 8*c* and 8*d*), (iii) no response (Fig. 8*e*) and (iv) a complex response (Fig. 8*f*). The direct response is generally only observed for relatively small grains, while the delayed response is dominant for relatively large grains. In a limited number of cases the transformation does not lead to a noticeable change in lattice parameter (Fig. 8*e*). As an example of the least frequent complex behaviour a two-step transformation was observed (Fig. 8*f*).

4.3. Martensite nucleation

The transformation start time for single austenite grains reflects the chance of nucleation for martensite plates. It is found that the martensite nucleation rate is controlled by two exponential contributions (San Martin *et al.*, 2010):

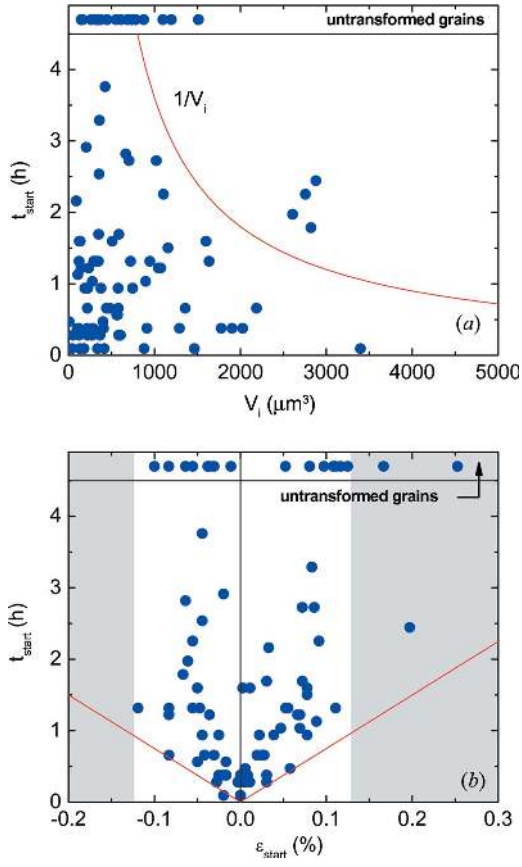

Figure 9
Transformation start time t_{start} of the monitored individual austenite grains during the martensite formation as a function of (*a*) the initial austenite volume V_i and (*b*) the strain in the austenite grain prior to the start of the transformation ε_{start}. The transformation is probed at 233 K in a magnetic field of 8 T. In (*a*) the curved line refers to the prediction for volume nucleation (see text). In (*b*) the inclined lines (red in the electronic version of the journal) indicate the maximum observable strain caused by martensite formation in neighbouring grains and the grey bands mark the critical strain for martensite nucleation. For comparison the untransformed grains after 4 h are also shown at the top of the graphs.

$$\frac{dN_{\alpha'}}{dt} = N_0 \nu \exp\left[-\frac{\Delta G^*(T,H)}{RT}\right] \exp\left(-\frac{Q}{RT}\right). \qquad (1)$$

The first exponential term is the driving force for the nucleation with ΔG^* referring to the energy barrier for nucleation, and the second exponential term is a mobility term for dislocation movement with an activation energy Q. The driving force causes a strong acceleration at lower temperatures, while the mobility term causes a deceleration, resulting in the characteristic C curve for the isothermal martensite transformation kinetics. The prefactor N_0 is the concentration of potential nucleation sites, R is the gas constant, T is the temperature and ν is the attempt frequency.

In Fig. 9 the transformation start time is shown as a function of the initial volume and the strain accumulated prior to the transformation for about 100 analysed single austenite grains. The data show that the larger grains tend to transform earlier than the smaller grains, suggesting that for larger austenite grains martensite nucleation has a higher probability. Considering the martensite nucleation rate of equation (1) we find that the martensite nucleation time can be characterized by a time constant of the form $\tau = (1/V_{\alpha'} N_0 \nu) \exp[(\Delta G^* + Q)/RT]$ (San Martin *et al.*, 2010). For an isothermal transformation the time to form the first martensite plate should scale with the inverse of the number of potential nucleation sites ($\tau \propto 1/N_0$). For nucleation with an equal probability for each point within the grain we expect $t_{start} \propto \tau \propto 1/V$. The nucleation of martensite plates is generally considered to be a heterogeneous process (Porter *et al.*, 2009). The critical nucleus is only a few nanometres in size and is expected to be strongly affected by the local dislocation structure (San Martin *et al.*, 2010).

The elastic strain developed prior to the transformation seems to promote the martensite nucleation for both compressive and tensile strains. The single-grain data indicate that no strain values are observed beyond a critical strain of about 0.12%. For short times this is logical as the nontransforming grains first need to develop a strain caused by martensite formation of neighbouring grains [indicated by the inclined lines in Fig. 9(*b*)]. For times beyond 1 h the development of elastic strains is expected to continue but seems to be limited to a (positive and negative) strain level of about 0.12%. This suggests that martensite nucleation is assisted by the elastic strain energy.

Besides the martensite start time t_{start}, it is interesting to consider the transformation time Δt to complete the martensitic transformation of individual austenite grains. In Fig. 10 a histogram of the transformation times is shown for the 71 grains that showed a complete transformation. The transformation time roughly follows a lognormal distribution with an average value of $\langle \Delta t \rangle = 0.87$ h ($\sigma_{\Delta t} = 0.51$ h). The observed transformation times are remarkably slow and support our previous findings that in this maraging steel there is no significant autocatalytic effect to accelerate the martensite nucleation (San Martin *et al.*, 2008). The relatively large fraction of monitored grains that are found to transform completely within 4 h indicates that the larger grains transform more easily than the smaller ones (the average size of the analysed grains is about 11 µm, while the average size from optical microscopy amounts to 7 µm).

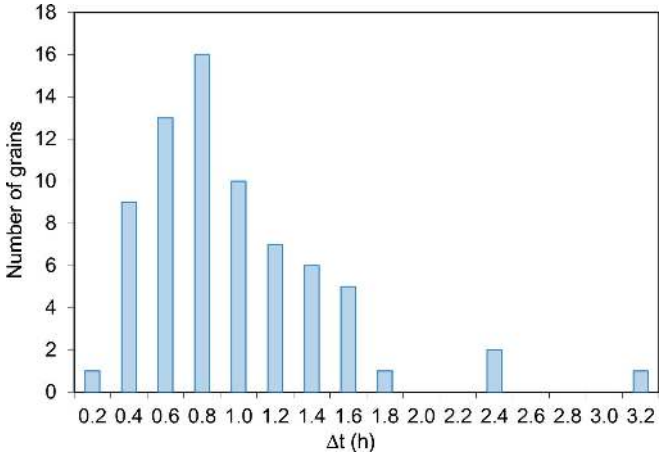

Figure 10
Distribution of the transformation time to complete the martensitic transformation (Δt) for the individual austenite grains.

4.4. Development of elastic strains in transforming austenite grains

In Fig. 11 the development of the elastic strain in a transforming austenite grain is shown as a function of the relative austenite volume. In order to qualitatively describe the observed behaviour a rather simplified model for the strain development in transforming austenite grains will be presented. A rigorous analysis involves the calculation of the anisotropic elastic response of the full local microstructure, which is beyond the scope of this work.

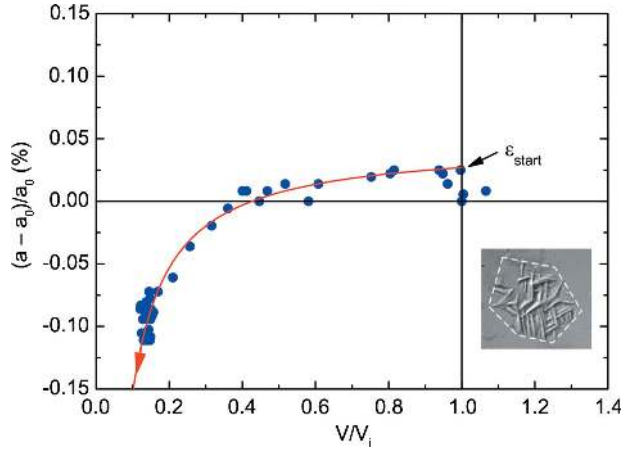

Figure 11
Development of the elastic strain in an individual austenite grain as a function of the relative austenite volume during the isothermal martensite formation at 233 K in a magnetic field of 8 T. Prior to the transformation a tensile strain develops as a result of the martensite formation in neighbouring grains (ε_{start}). During the martensite formation inside the austenite grain a compressive transformation strain develops. The curve indicates a model fit (see text).

The minimal ingredients required to qualitatively describe the strain development within a single austenite grain are (i) the volume change in the forming phase and (ii) partial confinement of this volume change by the surrounding matrix. As a starting point we can consider a single austenite grain that conserves its volume during the martensitic transformation. Assuming negligible compressibility of the martensite, the transformation strain for the untransformed austenite results directly from the change in volume between austenite and martensite. Volume conservation corresponds to $V_\gamma + V_{\alpha'} = V_0$, indicating that during transformation the untransformed austenite volume V_γ and the martensite volume $V_{\alpha'}$ are equal to the initial austenite volume V_0. Relaxation of the macroscopic strain corresponds to $\varepsilon_{V,\gamma} V_\gamma + \Delta\varepsilon_V V_{\alpha'} = 0$, where $\varepsilon_{V,\gamma}$ is the volume strain in the untransformed austenite volume and $\Delta\varepsilon_V$ = 2.1% is the difference in volume between martensite and austenite. For ideal volume conservation (full confinement) of the original grain the volume strain in the austenite phase corresponds to

$$\varepsilon_{V,\gamma} = -\Delta\varepsilon_V \left(\frac{V_0 - V_\gamma}{V_\gamma}\right). \quad (2)$$

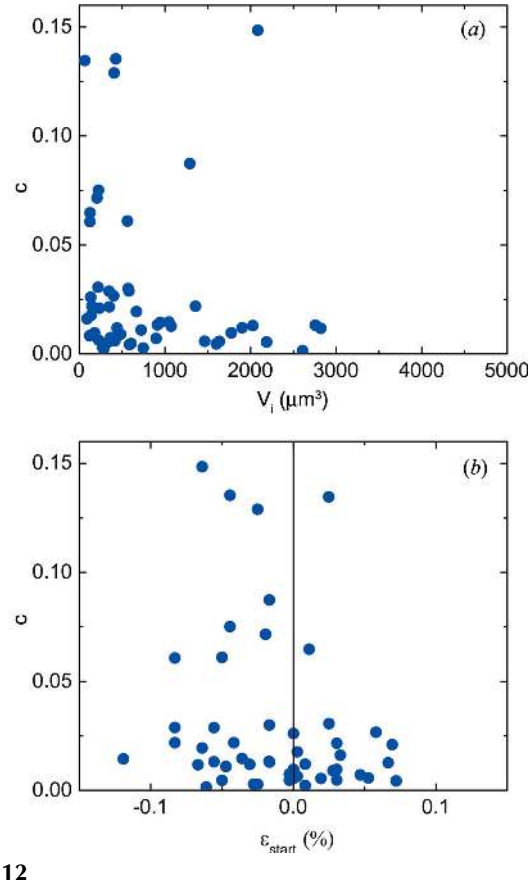

Figure 12
Strain confinement parameter c for the evolution of the linear transformation strain $\varepsilon_\gamma = -c(\Delta\varepsilon_V/3)(V_0 - V_\gamma)/V_\gamma$ of the monitored individual austenite grains during the martensite formation as a function of (*a*) the initial austenite volume V_i and (*b*) the strain in the austenite grain prior to the start of the transformation ε_{start}. The volume change between the martensite and the austenite amounts to $\Delta\varepsilon_V$ = 2.1%. The transformation is probed at 233 K in a magnetic field of 8 T.

Generalization suggests that for a partial strain confinement the linear transformation strain ($\varepsilon = \varepsilon_V/3$) in the austenite volume within the grain can be estimated by

$$\varepsilon_\gamma = -c\left(\frac{\Delta\varepsilon_V}{3}\right)\left(\frac{V_0 - V_\gamma}{V_\gamma}\right) = -c\left(\frac{\Delta\varepsilon_V}{3}\right)\left(\frac{1 - V_\gamma/V_0}{V_\gamma/V_0}\right), \quad (3)$$

where ε_γ is the transformation strain in the untransformed austenite, and c is a constant that describes the degree of strain confinement within the monitored grain ($0 \le c \le 1$). For a low value of c most of the transformation strain has relaxed to the surrounding matrix. As shown in Fig. 11 this simple model for partial strain confinement of the transformation strain gives a good description of the data. For the represented grain the constant c is about 0.03, indicating that 97% of the potential transformation strain is relaxed into the surrounding matrix. Within the presented model the constant c is merely an adjustable phenomenological parameter. In a more rigorous treatment the strain confinement of the transformation strain follows directly from the elastic response of the full microstructure.

In Fig. 12 the fitted strain confinement parameter c for the transformation of individual austenite grains is plotted as a function of the austenite volume and the initial strain at the start of the isothermal martensite transformation. For the larger grains only low c constants are observed, while for smaller grains a larger spread is observed extending to significantly larger c constants. This indicates that smaller grains have a higher potential for confinement of the transformation strain. Similarly, we observe that a compressive strain at the start of the transformation leads to a higher potential for strain confinement than an initial tensile strain.

5. Conclusions

We have performed time-resolved high-energy X-ray diffraction measurements on the isothermal martensite transformation of maraging steel in high magnetic fields. The main conclusions of these *in situ* studies are as follows:

(1) A magnetic field of 8 T strongly accelerates the isothermal martensite transformation at the nose temperature for the *C*-curve kinetics (233 K).

(2) The average phase behaviour demonstrates that the martensite formation does not lead to a macroscopic phase strain in the untransformed austenite.

(3) An analysis of individual reflections in the two-dimensional microbeam diffraction patterns indicates that single austenite grains do develop a transformation strain due to the formed martensite, which can be described by a partial strain confinement.

(4) The martensite nucleation is correlated with the austenite grain characteristics like the initial austenite volume and the strain developed prior to the transformation. The martensite start time tends to be reduced for larger grains, indicating volume nucleation at favourable dislocation configurations, while elastic strains (both compressive and tensile) seem to promote martensite nucleation.

(5) The time to completely transform individual austenite grains into martensite can be described by a lognormal distribution.

We acknowledge the European Synchrotron Radiation Facility for provision of synchrotron radiation facilities and thank the beamline staff for assistance in using beamline ID15A. This work was financially supported in part by the Foundation for Fundamental Research on Matter of the Netherlands Organization for Scientific Research, the Netherlands Institute for Metals Research currently known as the Materials Innovation Institute, the Spanish Ministerio de Economía y Competitividad (project No. MAT2010-19522), and the Engineering and Physical Sciences Research Council of the UK under grant No. GR/S44211.

References

Borgenstam, A. & Hillert, M. (1997). *Acta Mater.* **45**, 651–662.
Enomoto, M., Guo, H., Tazuke, Y., Abe, Y. R. & Shimotomai, M. (2001). *Metall. Mater. Trans. A*, **32**, 445–453.
Ghosh, G. & Olson, G. B. (1994). *Acta Metall. Mater.* **42**, 3371–3379.
Guo, H. & Enomoto, M. (2000). *Mater. Trans. JIM*, **41**, 911–916.
Hammersley, A. P., Svensson, S. O., Hanfland, M., Fitch, A. N. & Hausermann, D. (1996). *High Pressure Res.* **14**, 235–248.
Hedström, P., Lienert, U., Almer, J. & Odén, M. (2007). *Scr. Mater.* **56**, 213–216.
Holmquist, M., Nilsson, J.-O. & Hultin Stigenberg, A. (1995). *Scr. Metall. Mater.* **33**, 1367–1373.
Iqbal, N., van Dijk, N. H., Offerman, S. E., Moret, M. P., Katgerman, L. & Kearley, G. J. (2005). *Acta Mater.* **53**, 2875–2880.
Jaramillo, R. A., Babu, S. S., Ludtka, G. M., Kisner, R. A., Wilgen, J. B., Mackiewicz-Ludtka, G., Nicholson, D. M., Kelly, S. M., Murugananth, M. & Bhadeshia, H. K. D. H. (2005). *Scr. Mater.* **52**, 461–466.
Jeffries, J. R., Blobaum, K. J. M., Wall, M. A. & Schwartz, A. J. (2009*a*). *Phys. Rev. B*, **80**, 094107.
Jeffries, J. R., Blobaum, K. J. M., Wall, M. A. & Schwartz, A. J. (2009*b*). *Acta Mater.* **57**, 1831–1842.
Jimenez-Melero, E., van Dijk, N. H., Zhao, L., Sietsma, J., Offerman, S. E., Wright, J. P. & van der Zwaag, S. (2007). *Scr. Mater.* **56**, 421–424.
Jimenez-Melero, E., van Dijk, N. H., Zhao, L., Sietsma, J. & van der Zwaag, S. (2007). *Adv. X-ray Anal.* **51**, 69–75.
Joo, H. D., Kim, S. U., Shin, N. S. & Koo, Y. M. (2000). *Mater. Lett.* **43**, 225–229.
Kakeshita, T., Kuroiwa, K., Shimizu, K., Ikeda, T., Yamagishi, A. & Date, M. (1993*a*). *Mater. Trans. JIM*, **34**, 415–422.
Kakeshita, T., Kuroiwa, K., Shimizu, K., Ikeda, T., Yamagishi, A. & Date, M. (1993*b*). *Mater. Trans. JIM*, **34**, 423–428.
Kurdjumov, G. V. & Maksimova, O. P. (1948). *Dokl. Akad. Nauk SSSR*, **61**, 83–86.
Kurdjumov, G. V. & Maksimova, O. P. (1950). *Dokl. Akad. Nauk SSSR*, **73**, 95–98.
Kustov, S., Salas, D., Santamarta, R., Cesari, E. & Van Humbeeck, J. (2010). *Scr. Mater.* **63**, 1240–1243.
Lai, J. K. L., Shek, C. H., Shao, Y. Z. & Pakhomov, A. B. (2004). *Mater. Sci. Eng. A*, **379**, 308–312.
Lee, Y.-H., Todai, M., Okuyama, T., Fukuda, T., Kakeshita, T. & Kainuma, R. (2011). *Scr. Mater.* **64**, 927–930.
Offerman, S. E., van Dijk, N. H., Sietsma, J., Grigull, S., Lauridsen, E. M., Margulies, L., Poulsen, H. F., Rekveldt, M. Th. & van der Zwaag, S. (2002). *Science*, **298**, 1003–1005.
Ohtsuka, H., Xu, Y. & Wada, H. (2000). *Mater. Trans. JIM*, **41**, 907–910.
Pee, J.-H., Tada, M. & Hayakawa, M. (2006). *Mater. Sci. Eng. A*, **438–440**, 379–382.
Porter, D. A., Easterling, K. E. & Sherif, M. Y. (2009). *Phase Transformations in Metals and Alloys.* Boca Raton: CRC Press.
Rivoirard, S., Gaucherand, F., Bouaziz, O., Pinto Da Costa, E. & Beaugnon, E. (2006). *ISIJ Int.* **46**, 1274–1276.
Rodríguez-Carvajal, J. (1993). *Physica B*, **192**, 55–69.
San Martin, D., Aarts, K. W. P., Rivera-Diaz-del-Castillo, P. E. J., van Dijk, N. H., Brück, E. & van der Zwaag, S. (2008). *J. Magn. Magn. Mater.* **320**, 1722–1728.
San Martin, D., van Dijk, N. H., Jimenez-Melero, E., Kampert, E., Zeitler, U. & van der Zwaag, S. (2010). *Mater. Sci. Eng. A*, **527**, 5241–5245.
San Martin, D., Rivera Diaz del Castillo, P. E. J., Peekstok, E. & van der Zwaag, S. (2007). *Mater. Char.* **58**, 455–460.
Schnitzer, R., Zickler, G. A., Lach, E., Clemens, H., Zinner, S., Lippmann, Th. & Leitner, H. (2010). *Mater. Sci. Eng. A*, **527**, 2065–2070.
Servant, C., Bouzid, N. & Lyon, O. (1987). *Philos. Mag. A*, **56**, 565–592.
Slunder, C. J., Hoenie, A. F. & Hall, A. M. (1968). *Thermal, Mechanical Treatment for Precipitation-Hardening Stainless Steel*. Washington, DC: National Aeronautics and Space Administration.
Sordelet, D. J., Besser, M. F., Ott, R. T., Zimmerman, B. J., Porter, W. D. & Gleeson, B. (2007). *Acta Mater.* **55**, 2433–2441.
Staron, P., Jamnig, B., Leitner, H., Ebner, R. & Clemens, H. (2003). *J. Appl. Cryst.* **36**, 415–419.
Zhang, Y., He, C., Zhao, X., Esling, C. & Zuo, L. (2004). *Adv. Eng. Mater.* **6**, 310–313.
Zickler, G. A., Schnitzer, R., Hochfellner, R., Lippmann, Th., Zinner, S. & Leitner, H. (2009). *Int. J. Mater. Res.* **100**, 1566–1573.